# POSTSEISMIC DEFORMATION FOLLOWING THE 2010 HAITI EARTHQUAKE: TIME-DEPENDENT SURFACE SUBSIDENCE INDUCED BY GROUNDWATER FLOW IN RESPONSE TO A SUDDEN UPLIFT

**Shimon Wdowinski [(1)], Sang-Hoon Hong [(1)(2)]**

*[(1)] Division of Marine Geology and Geophysics, University of Miami*
*4600 Rickenbacker Cswy, Miami 33149, FL. U.S.A., shimonw@rsmas.miami.edu*
*[(2)] Satellite Data Application Department, Korea Aerospace Research Institute,*
*115 Gwahangno, Yuseong-Gu, Daejon, 305-333, Republic of Korea, shong@kari.re.kr*

## ABSTRACT

In this study we use Interferometric Synthetic Aperture Radar (InSAR) observations acquired by the TerraSAR-X (TSX) and the ALOS satellites to detect and characterize postseismic deformation induced by the 2010 Haiti earthquake. We obtained 8 TSX and 7 ALOS scenes covering the eastern portion of the earthquake rupture area, from before and after the earthquake. Interferometric data processing identified an elongated area of postseismic subsidence at the northeastern extent of the Leogane delta. The deformation is time-dependent and occurred in the first 45 days after the earthquake. We suggest that the deformation occurred due to sediment compaction in the near-coast end of the delta in response to groundwater flow, as the groundwater table adjusted to new hydraulic conditions imposed by the sudden uplift of the delta by 60-80 cm with respect to unchanged sea level. These observations suggest a new mode of postseismic deformation: it occurs in the very shallow part of the crust (upper few meters) and is very different from the other three known postseismic deformation mechanisms (afterslip, viscoelastic relaxation and poroelastic response), which occur within deeper crustal levels (1-30 kilometers).

## 1. INTRODUCTION

The 2010, M=7.0 Haiti earthquake was one of the worst natural disasters of the past century, with more than 300,000 fatalities, 400,000 injuries, and almost 2 million people homeless. The earthquake occurred near the Enriquillo Fault (Fig. 1), which accommodates part of the oblique convergence between the Caribbean and North American plates. Although the epicenter was located very close to the surface trace of the Enriquillo Fault, most of the rupture occurred on an inclined secondary fault [1, 2], which is part of the Haiti fault and thrust belt [3]. This 40 km long and 20 km deep fault segment, which lies beneath the Leogane delta, experienced both horizontal and vertical faulting with maximum slip of about 4 meters [1, 2]. The slip on the fault was arrested at a depth of about 2 km, resulting in null surface rupture. The only surface indicators for the earthquake are uplifted coral reefs and open fractures along some of the coastline [2].

Seismic energy release during an earthquake is part of a stress build-up and release process within the crust, which is often termed "the earthquake deformation cycle". The cycle includes the following three stages: stress build-up along active faults occurring over tens or hundreds of years (interseismic), sudden stress release by an earthquake (coseismic), and a stress re-adjustment stage occurring over a limited time period after the earthquake (postseismic). These stress changes induce crustal deformation that can be measured on the Earth's surface with geodetic instrumentation. The deformation measured during these three stages has different time characteristics. Interseismic deformation, which is driven by tectonic plate motion, is slow, typically in the order of a few mm/yr, and is time independent. Coseismic deformation occurs within a very short time and can reach maximum amplitude of several meters. Postseismic deformation is time dependent, typically highest right after the earthquake and its magnitude decays exponentially or logarithmically with time. The decay rate can vary significantly from one earthquake to the other, because transient postseismic deformation can occur by different deformation processes. The three known postseismic processes are afterslip, viscous relaxation, and poroelastic deformation [4] (Fig. 2).

In this study, we used Interferometric Synthetic Aperture Radar (InSAR) observations acquired by the TerraSAR-X (TSX) and the ALOS satellites to detect postseismic deformation induced by the 2010 Haiti earthquake. Both satellites detected an elongated area along the northern extent of the Leogane delta that underwent postseismic deformation. The elongated nature of the deformed area and its orientation parallel to the coastline are atypical for postseismic deformation, which usually occurs at the vicinity of the epicenter and follows the shape of the coseismic pattern. Here we characterize this unusual mode of postseismic deformation and provide a conceptual model for explaining the deformation, which we attribute to groundwater response to the sudden elevation change induced by the earthquake.

*Proc. 'Fringe 2011 Workshop', Frascati, Italy,*
*19–23 September 2011 (ESA SP-697, January 2012)*

## 2. DADA AND PROCESSING

We use both ALOS and TSX data to detect the coseismic and postseismic deformation induced by the 2010 Haiti earthquake. The two data sets complement one another in terms of coherence, coverage, and temporal resolution. The L-band ALOS data provide coherent interferograms, especially in vegetated areas, over wide swath (75 km wide). However, its 46-day repeat orbit does not provide sufficient temporal resolution to detect deformation changes over time that is needed for monitoring the time dependent postseismic deformation. Although the X-band TSX data is less coherent and acquired over a narrower swath (30 km), its 11-day repeat orbit provides critical observations for detecting the progression of the postseismic deformation with time.

We obtained a total of seven ALOS and three TSX scenes. Two of the ALOS scenes, one in ascending and the other in descending tracks, were acquired 1-2 years prior to the earthquake as part of the ALOS global acquisition plan. These two scenes combined with two post-earthquake scenes from two interferometric pairs that enable us to detect the coseismic deformation (Tab. 1). The other three ALOS senses were acquired 1, 47, and 93 days after the earthquake in a descending track. These three scenes are used to generate the three ALOS

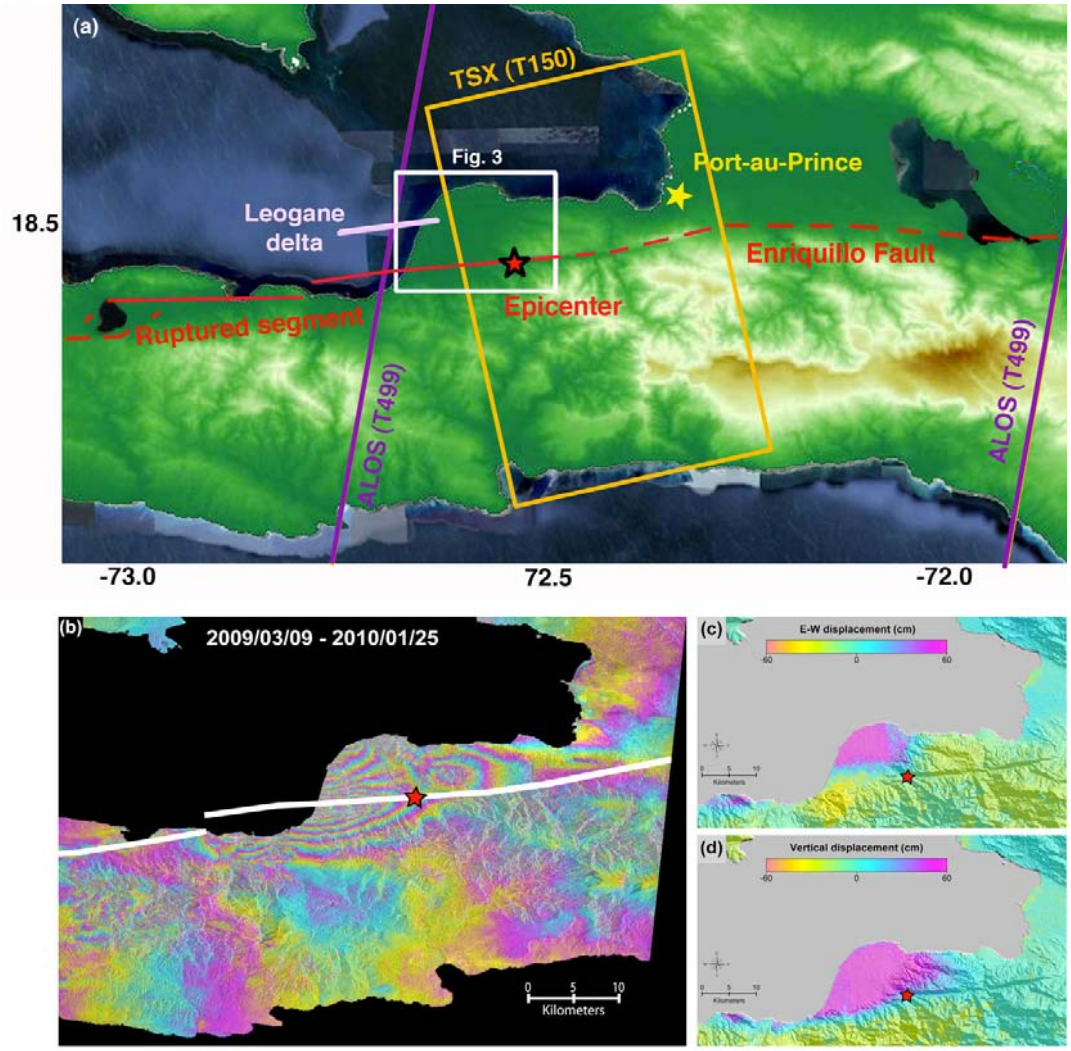


*Figure 1. (a ) SRTM-based elevation map of southern Haiti showing the location of the Enriquillo Fault and the epicentral location the 2010 Leogane earthquake. The white box marks the location of Fig. 3. The orange and purple boxes mark the swa thes of the TSX and ALOS data used for detecting the postseismic deformation. The background offshore imagery is obtained from Google Earth. (b) ALOS P ALSAR interferogram of the 2010 Leogane earthquake showing 12 cm con tours of ground displacement toward the satellite. This descending interferogram shows that most the surface displacement occurred west of the epicenter. (c) Vertical co-seis mic displacement derived from interferograms 20090309 – 20100125 (descending) and 20080209 – 20 100214 (ascending). Black star marks the epicenter location. (d) E-W horizontal co-seismic displacement derived from the same interferograms.*

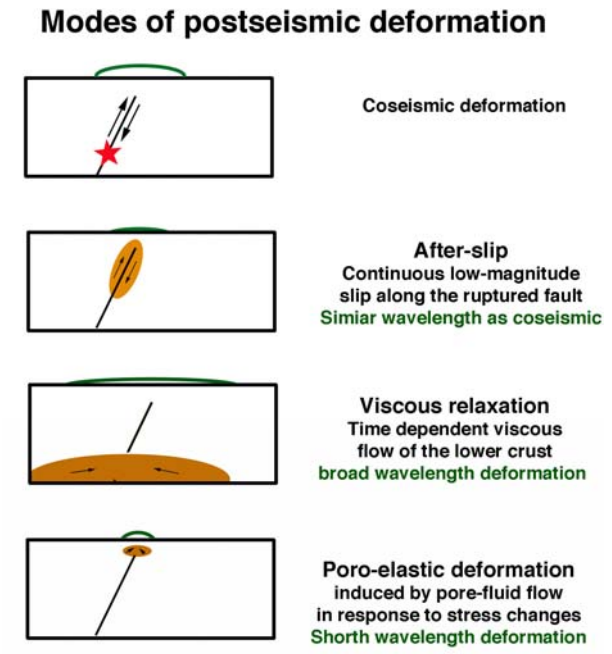


*Figure 2. Schematic illustration showing the postseismic deformation distribution within the crust (brown) and on the surface (green) that are induced by the three known postseismic deformation mechanisms.*

postseismic interferograms (Tab. 1). The three TSX scenes used in this study were acquired 2, 13, and 24 days after the earthquake in an ascending track and are used to generate the TSX postseismic interferograms (Tab. 1).

We processed the ALOS and the TSX data with the ROI_PAC software package [5]. The interferometric calculations include phase unwrapping [6], topographic phase removal based on the SRTM-1 DEM, and phase filtering [7]. All ALOS interferograms show a good coherence level, including the two coseismic interferograms with long temporal and long geometrical baselines (Tab. 1). The coherence level of the TSX interferogram is high for the two interferograms with 11-day temporal baselines (Fig. 3d and 3f) and somewhat lower for the 22-day temporal baseline (Fig. 3e). Despite the lower coherence level of the 22-day interferogram maintains sufficient phase allowing us the detection of the postseismic deformation.

## 3. RESULTS

The two ALOS coseismic interferograms were used by previous studies [1, 2] to characterize the coseismic deformation and infer slip distribution along the ruptured fault segments. Here we present only the descending one (Fig. 1b) to show the lateral extent of the coseismic deformation, which extends over a 40x20 $km^2$ area located mostly west of the epicenter. The interferogram shows that the earthquake affected the entire Leogane delta and other coastal areas further west. Although interferograms measure only changes along line of sight (LOS), a joint analysis of the ascending and descending interferograms allows the decomposition of both LOS information into vertical and E-W horizontal components [8]. Our decomposition analysis of the two coseismic interferograms reveals that the entire Leogane delta experienced both uplift and horizontal movements, both in the order of 60-80 cm (Fig. 1c and 1d).

Both ALOS and TSX postseismic interferograms show that the postseismic deformation occurred in a significantly smaller area than that of the coseismic deformation (Fig. 1 and 3).

*Table 1. Technical characteristics of ALOS and TSX interferograms.*

| No | Satellite | SAR image | | $B_{\perp}$ [1)] | $B_{temp}$ [2)] | *Additional information / Day after EQ* |
|---|---|---|---|---|---|---|
| | | Master | Slave | | | |
| 1 | ALOS | 2009-03-09 | 2010-01-25 | 820 m | 322 days | Coseismic -Decending |
| 2 | ALOS | 2008-02-09 | 2010-02-14 | 441 m | 735 days | Coseismic- Ascending |
| 3 | ALOS | 2010-01-13 | 2010-02-28 | 96 m | 46 days | 1-47 days |
| 4 | ALOS | 2010-01-13 | 2010-04-15 | 533 m | 92 days | 1-93 day |
| 5 | ALOS | 2010-02-28 | 2010-04-15 | 437 m | 46 days | 47-93 days |
| 6 | TSX | 2010-01-14 | 2010-01-25 | 99 m | 11 days | 2-13 days |
| 7 | TSX | 2010-01-14 | 2010-02-05 | 64 m | 22 days | 2-24 days |
| 8 | TSX | 2010-01-25 | 2010-02-05 | 35 m | 11 days | 13-24 days |

The coseismic deformation affected an elongated area, roughly 5x1 km$^2$, located along the northern shores of the Leogane delta. The ALOS interferograms show that the maximum deformation is less than a fringe, whereas the TSX interferograms show up to 4 fringes of deformation (Fig. 3). Despite the very different phase changes in the two interferogram types, both changes represent 6-7 cm of surface change in the line of sight (LOS), because a single L-band ALOS fringe reflects 12 cm of change, whereas a single X-band TSX fringe reflects 1.5 cm. The similar LOS change measured by TSX ascending track and ALOS descending track suggests that the deformation is mostly vertical, reflecting subsidence with maximum values of 10 cm near the shore.

The six postseismic interferograms, which measure surface change during different time windows after the earthquake, indicate that the deformation is time dependent. The two ALOS interferograms that use the 2010-01-13 acquisition, which was acquired 13 hours after the earthquake, show an overall similar phase change pattern (Fig. 3a and 3b), suggesting that most of the postseismic deformation occurred within the first 46 days after the earthquake. The third ALOS interferogram covering the period 47-93 days after the earthquake shows minor subsidence along the coast (Fig. 3c) suggesting that the postseismic subsidence continued after 46 days, but at a much slower rate.

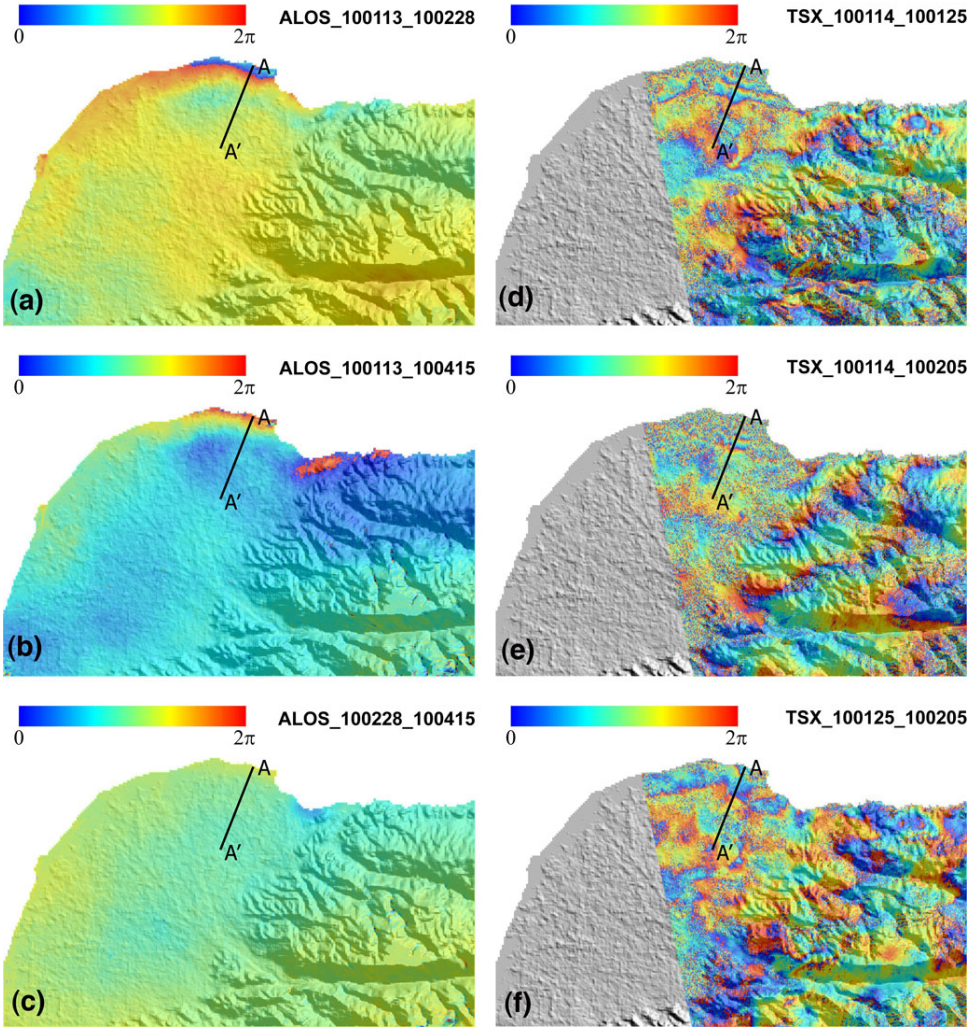


*Figure 3. ALOS and TSX interferograms of the Leogane delta showing phase change along the northern extent of the delta reflecting postseismic subsidence parallel to the delta's coastline. The TSX interferograms show 1-5 fringes reflecting 2-10 cm of subsidence, as a single fringe cycle of the X-band TSX represents 2 cm of vertical movement. The phase change in the ALOS interferograms are less than a fringe, but still represent up 10 cm of subsidence, because the single L-band fringe corresponds to 15 cm of vertical displacement. The six interferograms cover different time periods after the earthquake and, hence, capture different subsidence amount of this time dependent postseismic deformation. The black line marks the location of the subsidence profile shown in Fig. 4.*

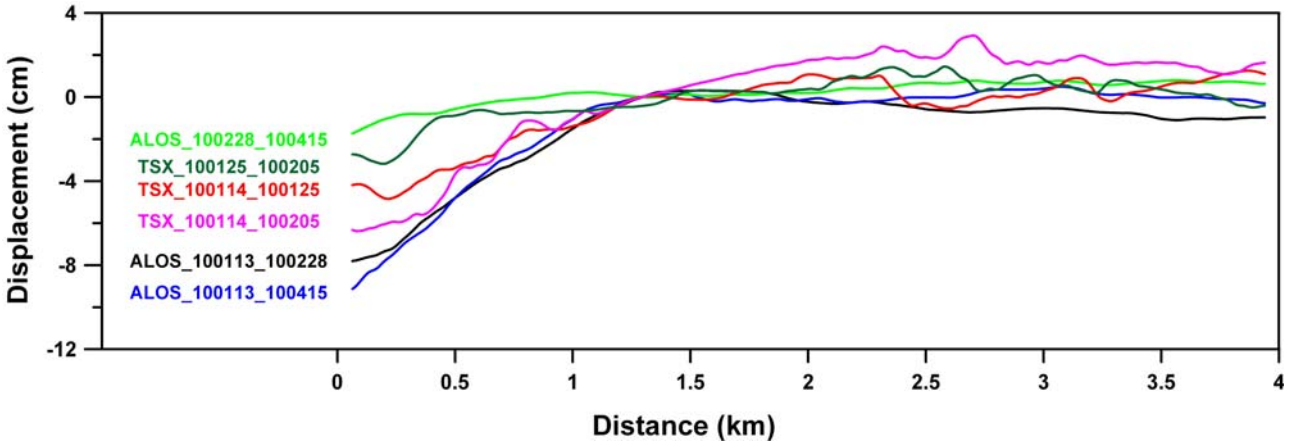


*Figure 4. A north-south profile showing subsidence changes with distance from the coastline as detected in the six postseismic interferograms. The interferogram and the profile location are presented in Fig 3. The four profiles with data acquired right after the earthquake (TSX_100114_100125, TSX_100114_100205, ALOS_100113_100228, and ALOS_100113_100415) show an increasing subsidence amount with the increasing interferogram time span (11, 22, 46 and 92 days). The other two interferograms (TSX_100125_100205 and ALOS_100228_100415) started subsidence more than 10 days after the earthquake and show limited subsidence, suggesting that most of the subsidence be occurred in the first 10 days.*

The three TSX interferograms, which cover the first 24 days after the earthquake, show more significant deformation changes with time. The two interferograms that share the 2010-01-14 acquisition, which were acquired 2 days after the earthquake, show a similar fringe pattern along the coast, but with a different number of fringes (Fig. 3d and 3e). The interferogram covering the first 13 days after the earthquake shows 3 fringes along the coast, whereas the interferogram covering the first 24 days shows 4 fringes. This observation suggests that the subsidence during the first 13 days was faster than in the subsidence afterward. The third TSX interferogram covering the time period 13-24 days after the earthquake shows only a single fringe along the coast (Fig. 3f), indicating that the subsidence indeed slowed with time.

The postseismic interferograms show that the subsidence is highest near the coast and decays inland. We plotted the subsidence as measured by the six interferograms along a single profile (A-A' in Fig. 3) oriented normal to the fringe direction. The subsidence profiles show an overall similar pattern of increased subsidence toward the coast, but at a different rate according to the time window covered by the interferogram (Fig. 4). The four profiles with data acquired right after the earthquake (TSX_100114_100125, TSX_100114_100205, ALOS_100113_100228, and ALOS_100113_100415) show an increasing subsidence amount with the increasing interferogram time span (11, 22, 46 and 92 days). The other two interferograms (TSX_100125_100205 and ALOS_100228_100415) started subsidence more than 10 days after the earthquake and show limited subsidence, suggesting that most of the subsidence be occurred within the first 13 days after the earthquake.

A synthesis of the postseismic interferograms suggests the following observations: (1) Deformation occurred in an elongated area along the northern extent of the Leogane delta and shows no relations to the coseismic deformation pattern or the epicenter; (2) The deformation reflects subsidence along and parallel to the coast only at the northern part of the delta; (3) The deformation is highest near the shoreline and decays inland; and (4) The deformation is time dependent; it was fastest right after the earthquake and slowed down as time passed. Most of the deformation (about 70 %) occurred in the first 13 days after the earthquake, additional 20 % in the following 11 days, and the rest of it (10 %) in the remaining 70 days.

## 4. CONCEPTUAL MODEL

The land subsidence observed along the northern extent of the Leogane delta following the 2010 Haiti earthquake is unusual postseismic deformation signal in terms of location, size, and pattern. The subsidence occurred in a narrow strip along the northern coast of the delta. Because it shows no resemblance to the coseismic deformation pattern and no relation to the epicentral location, it cannot be explained by any of the known postseismsic deformation mechanisms: afterslip, viscous relaxation, or poroelastic deformation (Fig. 2).

The narrow width (~1 km) and orientation parallel to the coast suggest that the observed postseismic subsidence reflects a shallow process induced by the earthquake along the coast. The most apparent changes along the Leogane delta's coast are uplifted corals indicating a 60-

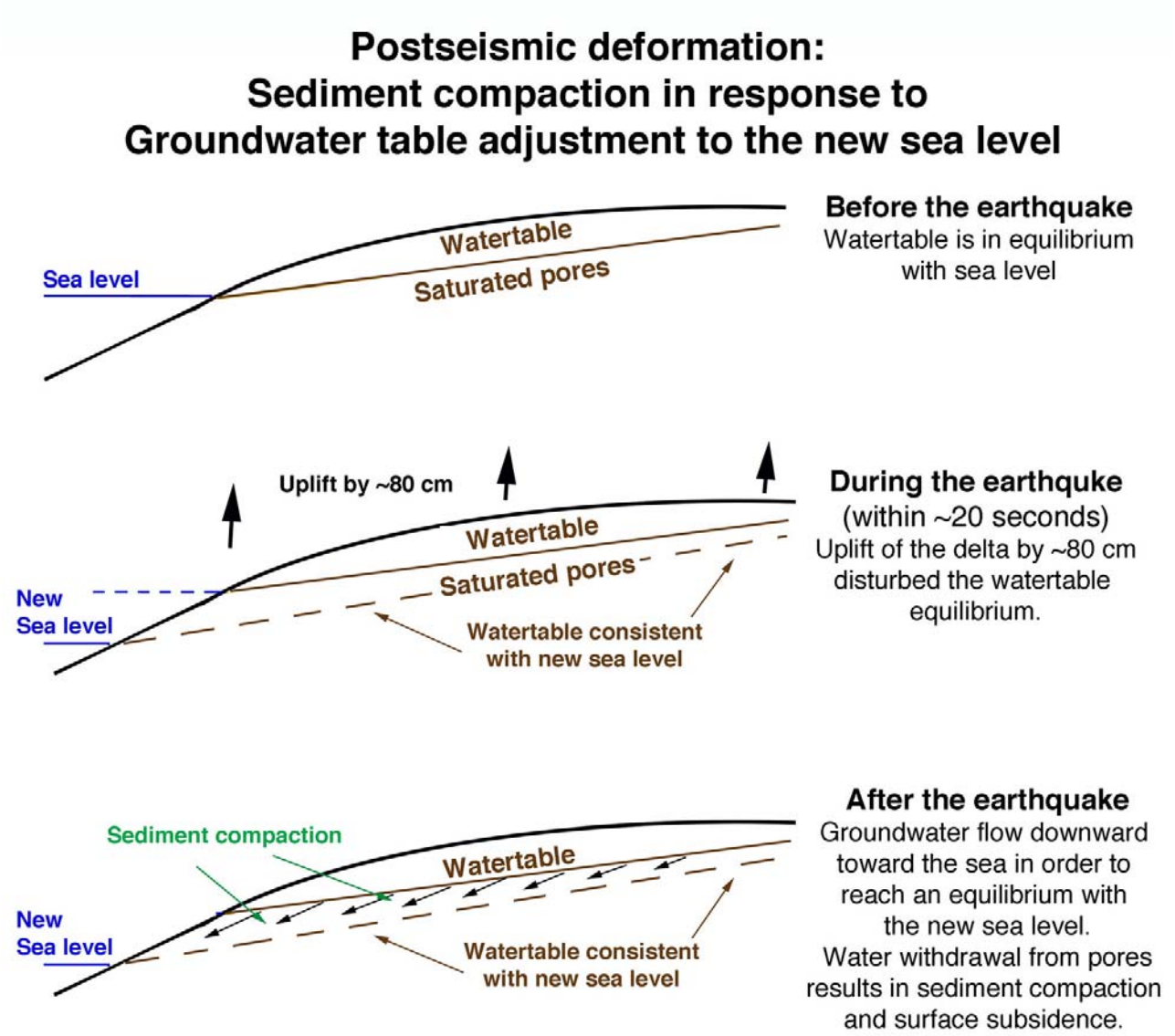


*Figure 5. Schematic illustration presenting the conceptual model for the observed subsidence along the northern shores of the Leogane delta following the 2010 Haiti earthquake.*

80 cm of coseismic uplift [2]. This coastal uplift is part of the overall 60-80 cm uplift of the entire Leogane delta measured by InSAR (Fig. 1d). Because sea level was not affected by the earthquake, the local effect of the coseismic uplift was a sudden sea level drop, which also exposed the corals to air. We postulate that the sudden sea level drop also affected the near coast onshore area and induced the observed postseismic subsidence.

We present a conceptual physical model that explains the observed postseismic subsidence along the Leogane delta by a sudden sea level drop induced by the earthquake. As indicated above, the earthquake didn't affect global sea level. The sudden sea level drop is the relative vertical land-sea motion in the delta reference frame. The model accounts for groundwater changes induced by the sudden sea level drop and sediment compaction in response to groundwater changes. The model has the following three stages (Fig. 5):

1) Pre-earthquake (interseismic) groundwater-sea level equilibrium (Fig. 5a). In coastal areas, groundwater level is determined by sea level and the coastal groundwater hydraulic head (pressure); the head drives freshwater toward the sea when it is positive or drives saltwater inland when negative. The hydraulic head in the Leogane delta is positive, as it serves an outlet for a large amount of surface runoff drained by Momance River. Therefore, the groundwater table elevation near the coast has a slight upward slope inland. Periodic changes in sea level or hydraulic head cause fluctuations in the

height and gradient of the groundwater level inland. Daily, tidal induced sea level sea level changes affect groundwater level only very close to the coast (several meters). Seasonal changes in the hydraulic head affect primarily the groundwater gradient, as the drainage base (sea level) remains unchanged. Overall, the inland upward inclined groundwater level represents equilibrium between the drainage base at sea level and the positive hydraulic head. Rocks (unconsolidated sediments) located beneath groundwater level are fully saturated, whereas rock located above that level are unsaturated.

2) Coseismic uplift: a sudden disruption of the groundwater-sea level equilibrium (Fig. 5b). The 2010 Haiti earthquake uplifted the Leogane delta by 60-80 cm within less than 20 seconds. In the delta's reference frame, it was a sudden drop of sea level by the same amount, which left many exposed corals along the delta's shores. This sudden drop of sea level disrupted the previous equilibrium between groundwater and sea level. Almost instantaneously, the drainage base of the groundwater was lowered by 60-80 cm. This resulted in a 60-80 cm thick layer of saturated unconsolidated sediments located between the pre-earthquake groundwater level and the new groundwater equilibrium level.. Groundwater below the new equilibrium level remained in equilibrium and, hence, was not affected by the earthquake.

3) Postseismic equilibrium re-adjustment: groundwater flow and sediment compaction (Fig. 5c). The 60-80 cm thick layer of saturated with water located above the new equilibrium level responded to the sudden sea level drop by horizontal and downward flow toward the new drainage base. Because groundwater flow occurs through a resistive medium (unconsolidated sediments), the adjustment to the new drainage base is not instantaneous, but occurs over time. It is a time-dependent process that can be modeled as a diffusion flow theory applicable to groundwater flow, i.e., Darcy's equation. The initial flow is fast and occurs only near the shore. With time, the re-adjustment process propagates further inland but occurs at slower flow rates. Groundwater withdrawal from the 60-80 cm thick layer of unconsolidated sediments induces sediment compaction. Reduction of pore pressure leads to better and more compact arrangement of the sediments, which results in surface subsidence. An estimate for the amount of compaction can be obtained from the InSAR observations, by dividing the maximum subsidence (10 cm, Fig. 4) by the coseismic uplift (60-80 cm, Fig. 1d). This simple calculation suggests 12-17% of compaction due to groundwater withdrawal.

## 5. DISCUSSION AND CONCLUSIONS

We used three X-band TSX interferograms and three L-band ALOS interferograms to detect and characterized time dependent deformation following the 2010 Haiti earthquake. Both observation types detected an elongated area located at the northern extent of the Leogane delta that experienced subsidence right after the earthquake. The subsidence is highest near the delta's shores and decays inland within a distance of about 1 km. Thanks to the 11 day TSX repeat orbit, we were able to characterize the time dependency of the deformation, which was faster during the first 13 days after the earthquake, slowed down in the following 11 days, and almost ceased after 47 days. The observed postseismic subsidence show no resemblance to the coseismic deformation pattern and no relations to the epicenter of the 2010 Haiti earthquake. Therefore it cannot be explained by the three known modes of postseismic deformation, which are afterslip, viscous relaxation and poroelastic deformation.

We suggest that the observed subsidence following the 2010 Haiti earthquake represent a new mode of postseismic deformation occurring very close to the surface by sediment compaction in response to groundwater level changes induced by the sudden coseismic uplift of the Leogane delta. We explain the observed subsidence using a conceptual model that has the following three stages: (1) Pre-earthquake (interseismic) groundwater-sea level equilibrium; (2) Coseismic uplift: a sudden disruption of the groundwater-sea level equilibrium; and (3) Postseismic equilibrium re-adjustment: groundwater flow and sediment compaction. The model explains the elongated shape of the postseismic subsidence signal along the coast, as well as the time dependence characteristics of the deformation.

In this study we used both ALOS and TSX observations to detect subsidence following the 2010 Haiti earthquake. The two observation types complement one another, as the L-band ALOS data is acquired over a wider swath and maintain higher interferometric coherence level, whereas the 11 day repeat orbit of the X-band TSX provide critical observations for characterizing the time dependence subsidence. We were able to use both sensors to characterize the postseismic deformation, because both operating space agencies, DLR (TSX) and JAXA (ALOS), responded quickly to the Haiti earthquake and started monitoring the earthquake's damaged area within 1-2 days after the earthquake. Both agencies continued acquiring data along the same tracks in the following weeks and months, which was critical for generating interferograms. It will be useful to apply such rapid response after other large magnitude earthquake, in order to continue detecting various modes of postseismic deformation.

The detection of postseismic deformation is also important for more accurate assessments of the coseismic deformation signal. Because postseismic deformation started right after the earthquake, coseismic interferograms spanning from before the earthquake till several weeks after the earthquake (Tab. 1) are contaminated by the postseismic signal. Thus, the coseismic deformation of the 2010 Haiti earthquake has been locally under-estimated (up to ~15%) due to the unaccounted postseimic subsidence. A more careful assessment of the Haiti coseismic signal should correct the observations for unaccounted postseismic subsidence.

## ACKNOLEDGEMENT

This work was enabled by the TSX science proposal (GEO0746). We also thank JAXA for access to ALOS data. The research was supported by NSF award No. 1037930 (RAPID: Monitoring Postseismic Crustal Deformation in Haiti with TerraSAR-X Observations). We thank Fernando Miralles-Wilhelm and Tim Dixon for their very useful suggestions.

## REFERENCES

1. Calais, E., A. Freed, G. Mattioli, F. Amelung, S. Jonsson, P. Jansma, S.H. Hong, T. Dixon, C. Prepetit, and R. Momplaisir (2010): Transpressional rupture of an unmapped fault during the 2010 Haiti earthquake, *Nature Geoscience,* **3**(11), 794-799.
2. Hayes, G.P., R.W. Briggs, A. Sladen, E.J. Fielding, C. Prentice, K. Hudnut, P. Mann, F.W. Taylor, A.J. Crone, R. Gold, T. Ito, and M. Simons (2010): Complex rupture during the 12 January 2010 Haiti earthquake, *Nature Geoscience,* **3**(11), 800-805.
3. Pubellier, M., J.M. Vila, and D. Boisson (1991): North Carabbean neotectonic events - The trans-Haitian fault system - Tertiary record of an oblique transcurrent shear zone uplifted in Hispaniola, *Tectonophysics,* **194**(3), 217-236.
4. Barbot, S. and Y. Fialko (2010): A unified continuum representation of post-seismic relaxation mechanisms: semi-analytic models of afterslip, poroelastic rebound and viscoelastic flow, *Geophysical Journal International,* **182**(3), 1124-1140.
5. Buckley, S.M., P.A. Rossen, and P. Persaud (2000): ROI_PAC Documentation - Repeat Orbit Interferometry Package.,
6. Chen, C.W. and H.A. Zebker (2001): Two-dimensional phase unwrapping with use of statistical models for cost functions in nonlinear optimization, *Journal of the Optical Society of America a-Optics Image Science and Vision,* **18**(2), 338-351.
7. Goldstein, R.M. and C.L. Werner (1998): Radar interferogram filtering for geophysical applications, *Geophysical Research Letters,* **25**(21), 4035-4038.
8. Fialko, Y., M. Simons, and D. Agnew (2001): The complete (3-D) surface displacement field in the epicentral area of the 1999 M(w)7.1 Hector Mine earthquake, California, from space geodetic observations, *Geophysical Research Letters,* **28**(16), 3063-3066.